Journal of Molecular Liquids xxx (xxxx) xxx

Contents lists available at ScienceDirect

Journal of Molecular Liquids

journal homepage: www.elsevier.com/locate/molliq

Effect of supramolecular polymeric aggregation in room temperature ionic liquids (RTILs) on catalytic activity in the synthesis of *4H*-chromene derivatives and Knoevenagel condensation

Shoaib Muhammad [a], Firdous Imran Ali [a,*], Muhammad Naveed Javed [a], Agha Arsalan Wasim [a], Ahmed Bari [b], Faisal Rafique [c], Muhammad Amjad Ilyas [c], Kashif Riaz [a,c], Syed Junaid Mahmood [d], Amir Ahmed [d], Imran Ali Hashmi [a,*]

[a] *Department of Chemistry, University of Karachi, Main University Road, Karachi 75270, Sindh, Pakistan*
[b] *Department of Pharmaceutical Chemistry, College of Pharmacy, King Saud University, P.O. Box 2457, Riyadh 11451, Saudi Arabia*
[c] *Department of Applied Physics, University of Karachi, Main University Road, Karachi 75270, Sindh, Pakistan*
[d] *PCSIR Labs Complex, Karachi 75280, Pakistan*

ARTICLE INFO

Article history:
Received 3 July 2020
Received in revised form 21 September 2020
Accepted 1 October 2020
Available online xxxx

Keywords:
Supramolecular polymeric aggregation
Ionic liquids
4H-chromene
Knoevenagel condensation

ABSTRACT

RTILs exhibit supramolecular self-assembled polymeric aggregation due to noncovalent interactions. The influence of the aggregation behaviour of RTILs on catalytic activity is evident but still poorly understood. The present work focuses on establishing a relationship between the role of supramolecular self-assembly of RTILs on catalysis in organic reactions. Herein, we report four unreported, air and water stable, halide free, C_2-symmetrical, third generation, hydrophobic imidazolium-based room temperature ionic liquids (**RTILs 1–4**), their synthesis and function as catalysts for the synthesis of *4H*-chromene derivatives (terahydrobenzo[*b*]pyran) and Knoevenagel condensation. The RTILs showed unprecedented solubility/miscibility behaviour. The RTILs showed that *1,3-dihexylimidazolium 2-aminobenzoate* [hhim][OAB] (**RTIL-3**) performed better in terms of yield and reaction time. Supramolecular polymeric aggregation was explored by employing ESIMS, while the critical aggregation concentration (CAC) was calculated via recording electrical conductivity of RTILs in absolute ethanol. We have also used rheometry experiments to explore forces governing the occurrence of aggregates in the liquid phase of RTILs.

1. Introduction

Self-assembly of molecules due to non-covalent (H-bonding, π-π stacking ionic interactions, van der Waal's forces, etc.) generates supramolecular polymeric aggregates/clusters. The influence of supramolecular polymeric self-assembly or material assembly (especially ionic liquids) on catalysis is a neglected topic and is still in its infancy. Llansola et al. observed remarkable differences in the catalytic activity of two different catalysts, out of which only one showed supramolecular polymeric aggregation [1]. Ionic liquids, especially imidazolium-based ionic liquids, are considered self-assembled solvents that can accommodate guest organic molecules by creating cavities and hence provide an excellent platform for catalysis. Not only the dramatic boost in the rate of those reactions involving charge-separated intermediates or transition states observed due to imidazolium-based ionic liquids but also a considerable influence on the reaction mechanism has been suggested [2,3]. The effect of noncovalent interactions (H-bonding, electrostatic forces, π-π stacking, etc.) on the catalytic activity of various reactions including, acetlylation reaction [4], esterification [5], Friedel-crafts reaction, and other nucleophilic aromatic substitution reactions [6,7], the multicomponent Biginelli reaction [8], the Baylis-Hillman reaction [9] and N-formylation [10] etc. The role of supramolecular self-assembly on the catalytic activity of RTILs in chemical reactions is not well established or numeric. Hence, for precise applications of ILs as catalysts, there is a need of a better understanding of the relationship between this behaviour of RTILs and its effect on catalytic activity.

We previously reported the catalytic activity of hydrophilic ionic liquids for C—C bond forming reactions and explored the relationship of supramolecular aggregation of imidazolium ionic liquids based on catalytic activity [11,12]. In continuation of our studies, herein, we report the catalytic activity of hydrophobic **RTILs 1–4** on the synthesis of *4H*-chromene derivatives and Knoevenagel condensation. Despite a huge number of published studies on chemical reactions in ILs, the use of hydrophobic ILs as catalysts, is rare. The catalytic activity of these new RTILs for the synthesis of *4H*-chromene derivatives (tetrahydrobenzo

---

* Corresponding authors.
E-mail addresses: firdous@uok.edu.pk (F.I. Ali), iahashmi@uok.edu.pk (I.A. Hashmi).

https://doi.org/10.1016/j.molliq.2020.114503
0167-7322/

Please cite this article as: S. Muhammad, F.I. Ali, M.N. Javed, et al., Effect of supramolecular polymeric aggregation in room temperature ionic liquids (RTILs) on catalyti..., Journal of Molecular Liquids, https://doi.org/10.1016/j.molliq.2020.114503

[*b*]pyran) and the C—C bond forming reaction was investigated. The *4H*-chromene was selected not only because it presents an important structural motif and biologically significant class of compounds but also because of the cascading C—C bond forming reactions through which it proceeds such as Knoevenagel condensation and Michael addition followed by heterocyclization [13]. Knoevenagel condensation is an important C═C bond forming reaction that furnishes significant intermediates for a number of value-added materials but needs an environmentally benign protocol. The comparison of the present strategy is compared with previously reported methods in Table 5. In addition, the catalytic activity of RTILs **1–4** for the previously studied C—C bond forming reaction, Knoevenagel condensation, was also independently demonstrated.

By definition, RTILs are assemblies of ions such as salts melting below 100 °C [14]. These unique materials exhibit intrinsic physiochemical properties, including thermal stability and low vapor pressure. Due to these significant characteristics, these value-added materials have been utilized in different applications, some of which are solvents and catalysts in organic reactions [15–18], polymerization [19] and nanoparticle synthesis [20], separation methods for extraction of metal ions [21–23], plant materials [24,25] etc. and as electrolytes in batteries, fuel cells, dye sensitized solar cells [26,29,30], etc. and as thermal fluids for heat storage devices [31]. Over the past decade, the use of ionic liquids as catalysts and environmentally friendly solvent system as conventional volatile organic solvents in organic reactions has been well demonstrated [32,33]. The most commonly studied cations for ionic liquids are immidazolium, ammonium, phosphonium, pyridinium, piperidinium, pyrolidinium, etc. Due to the ease of synthesis, low viscosity and chemical and thermal stability, imidazolium is the most studied cation of ionic liquids [34–37].

Almost 40 years ago, John Wilkes et al. reported [38] chloride salts of 1,3-dialkyl imidazolium cations as first room temperature ionic liquids (RTILs). The discovery was followed by second generation (air and moisture stable RTILs) [39] and third generation (halide free) [40] ionic liquids. The purpose of designing second-generation ILs was to furnish an alternative medium for chemical reactions [41] considering the non-volatile feature of ILs Another key fact is the hydrophobic character, i.e., IL immiscibility with water can be attained by providing suitable anions/cations. Hydrophobicity is introduced to avoid water contamination.

Therefore, our first objective was to regulate the thermal stability and miscibility of RTILs by selecting appropriate ions. We selected imidazole to prepare 1,3-dihexyl imidazolium as a cation, while naturally occurring substituted aromatic carboxylates were selected as anions for two reasons: a) to avoid toxic halide and b) provide highly delocalized bulky anions to introduce hydrophobic character and lower viscosity (Fig. 1).

The behaviour and suitability of ILs for a number of applications depends upon their molecular level structure. Electron spray ionization mass spectrometry (ESI-MS) has been used to investigate supramolecular polymeric aggregation in newly prepared RTILs [41]. Furthermore, measurement of electrical conductivities is used to calculate the critical aggregation concentration (CAC) [42].

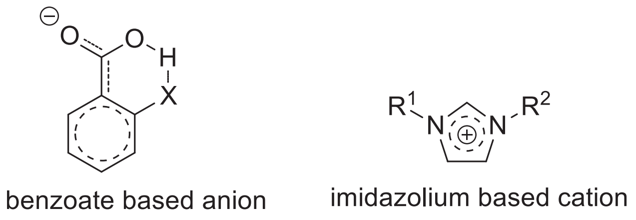

Fig. 1. Charge distribution in ions.

It has been reported that both ionic interactions and hydrogen bonding can cause aggregations in ionic liquids [43]. Aggregates formed due to hydrogen bonding tend to break easily and produce an effect that we call shear thinning, a property possessed by non-Newtonian fluids [44]. Since our ILs are all Newtonian, we can easily exclude this hypothesis of *hydrogen bonding* aggregation. Interionic interactions may also cause aggregation via ion pairing, however, there are two possibilities. Either the aggregate is overall neutral, or it is charged. It is reported that the former would lead to non-Newtonian behaviour [45]. Aggregates formed by ionic interactions possessing an overall charge are a preferable option that may be further supported by the evaluation of ionic structural charges participating in ion pairing and the overall charge of aggregates formed.

The, relationship between supra-molecular aggregation and catalytic performance in the chemical reactions of ionic liquids is hitherto unknown. Herein, we have also demonstrated the effect of aggregation behaviour of RTILs on the catalytic performance in the mentioned chemical reactions of C—C bond formation/heterocyclization.

2. Methods and materials

2.1. General

Oven dried glassware was utilized for all chemical reactions. All chemicals were purchased from Sigma-Aldrich and verified via thin layer chromatography (TLC) using precoated aluminium plates, Kieselgel 60, F254, 0.25 mm, e. Merck, Darmstadt, Germany and FTIR. To evaporate solvents, a rotary evaporator was used, maintaining 40 °C of the water bath. For visualization of chromatograms, iodine spray or UV lamp (254 nm) was used. FTIR was recorded on a Shimadzu spectrophotometer. Electron spray ionization mass Spectrometry (ESI-MS) was performed on an AB SCIEX QSTA R XL LCMSMS Q-Tof (pH 3.2, acetonitrile:water 1:1). ^{1}H NMR and ^{13}C NMR were obtained from an AVANCE AV-500, and AV-125 BRUKER. Electrical conductivity was measured on a Hanna (HI763100) conductivity meter. For melting point measurement, Stuart Digital Melting Apparatus SMP 10 was used. For rheology Brookfield DV-III rheometer with spindle 0 was used.

2.2. Synthesis of 1,3-dihexylimidazolium bromide ([hhim]$^+$ [Br]$^-$)

Then 29.4 mmol (1 equivalent) imidazole in 20 mL THF was added dropwise in an ice cooled solution of 29.4 mmol (1 equivalent) of powdered NaH in 20 mL THF. The imidazole solution was completely added, followed by stirring of the mixture for two hours at room temperature. First, 58.8 mmol (2 equivalents) 1-bromohexane was added dropwise, followed by refluxing of the mixture for eight and half hours. The reaction was monitored through TLC, and THF was evaporated under vacuum and [hhim]$^+$ [Br]$^-$ is extracted using dichloromethane (DCM) as a light brown waxy solid. Yield: 78% [46].

2.3. Synthesis of 1,3-dihexylimidazolium 2-hydroxybenzoate (RTIL-1)

A round bottomed flask containing 20 mmol *o*-hydroxybenzoic acid (**OHB**) and 22 mmol Na_2CO_3 (sodium bicarbonate) in 12 mL water was stirred at room temperature until neutralization was achieved (checked via litmus paper). Then, 19 mmol of [hhim]$^+$ [Br]$^-$ was added and stirring and continued for up to 30 min [46]. RTIL-1 is extracted with $CHCl_3$ (chloroform). The extracted RTIL-1 was dried and evaporated over a week under vacuum in the presence of a cold trap to obtain pure RTIL-1 as a waxy yellow and hydrophobic product. Yield: 90%.

IR ν_{max} KBr cm^{-1}: 3412.7 (phenolic OH), 3140.2, 3067.4 (aromatic C—H stretching), 2957.8, 2931.3, 2861.1 (aliphatic C—H stretching due to octyl chain hydrogen), 1629.8 (conjugated C═O), 1569.7 (C═N imidazole ring), 1464.2 (C═C imidazole ring), 1385.0 (C—O), 1167.4 (C—C).

***^{1}H NMR* (DMSO-d_6, 500 MHz) δ ppm:** 9.31 (s, H-2, 1H), 7.82 (s, H-4 and H-5, 2H), 7.65 (dd, $J = 8.0, 2.0$ Hz, H-2′ 1H), 7.11 (dd, $J = 8.0, 2.0$ Hz, H-4′ 1H), 6.59 (dd, $J = 8.0, 2.0$ Hz, H-3′, 1H), 6.57 (dd, $J = 8.0, 2.0$ Hz, H-5′, 1H), 3.83 (d, $J = 6.5$ Hz, N-CH$_2$, 4H), 1.79 (s, CH$_2$- CH$_2$N, 4H), 1.25 (broad singlet, CH$_2$ x 3, 6H), 0.85 (s, terminal CH$_3$ of alkyl chains attached to imidazolium moiety, 6H).

***^{13}C NMR* (DMSO-d_6, 125 MHz) δ ppm**: 171.7 (-COO$^-$), 163.5 (C-OH aromatic), 136.5 (N-C=N imidazole ring), 131.7 (Anion C—H, C-4′), 130.3 (Anion C—H, 6′), 122.9 (C-1′), 120.9 (Imidazole C-4 and C-5), 116.2 and 116.1 (Anion C—H, C-3′ and 5′), 49.3 (N-CH$_2$, C-1 of alkyl chain), 30.9 (CH$_2$, C-2 of alkyl chain), 29.7 (CH$_2$, C-3 of alkyl chain), 25.5 (CH$_2$, C-4 of alkyl chain), 22.3 (CH$_2$, C-5 of alkyl chain), 14.2 (Terminal CH$_3$, C-6 of alkyl chain).

HR-ESI-MS + ve: *m/z* 237.2224 (C+, **c**alcd. for $C_{15}H_{29}N_2^+$ *m/z* 237.2325), *m/z* 321.3290 (C^++Hexyl; $C_{21}H_{49}N_2^+$); *m/z* 153.1406 (C^+ − Hexyl; $C_9H_{17}N_2^+$); **HR-ESI-MS –ve:** *m/z* 137.0167 (calcd. For $C_7H_5O_3^-$ *m/z* 137.0238); *m/z* 93.0312 ($C_5HO_2^-$, A$^-$ - CO$_2$); *m/z* 511.2794 ([CA$_2$]$^-$, $C_{29}H_{39}N_2O_6^-$), *m/z* 885.5353 ([C$_2$A$_3$]$^-$, $C_{51}H_{73}N_4O_9^-$).

2.4. Synthesis of 1,3-dihexylimidazolium 4-hydroxybenzoate (RTIL-2)

Sodium salt of *p*-hydroxybenzoic acid (PHB) was prepared, followed by ion exchange with [hhim]$^+$ [Br]$^-$ following the method described in Section 2.3. A yellow-coloured waxy hydrophobic product was obtained. Yield: 90%.

IR ν_{max} KBr cm^{-1}: 3379.82 (phenolic OH), 3149.5, 3093.3 (aromatic C—H stretching), 2958.2, 2930.4, 2859.3 (aliphatic C—H stretching due to octyl chain hydrogen), 1611.6 (conjugated C=O), 1544.8 (C=N imidazole ring), 1425.9 (C=C imidazole ring), 1380.7 (C—O), 1165.2 (C—C).

***^{1}H NMR* (DMSO-d_6, 500 MHz) δ ppm:** 16.5 (H-bonding), 9.29 (s, N-CH-N, 1H), 7.82 & 7.62 (each s, H-4 & H-5 imidazole ring, 2H), 7.12 (s, H-2′ & H-6′, 2H), 6.60 (s, H-3′ & H-5′, 2H), 4.17 (s, N-CH$_2$, 4H), 1.79 (br. s, CH$_2$- CH$_2$N, 4H), 1.68, 1.26 (broad singlet, CH$_2$ x 6, 12H), 0.85 (s, terminal CH$_3$, 6H).

***^{13}C NMR* (DMSO-d_6, 125 MHz) δ ppm:** 163.4 (C-OH aromatic), 136.5 (N-C=N imidazole ring), 131.6 (Anion C—H, C-2′ & C-6′), 130.3 (Anion C—H, C-1′), 122.9 (imidazole C-4 & C-5), 116.2 (Anion C—H, C-3′ & C-5′), 49.3 (N-CH$_2$, C-1 of alkyl chain), 31.1 (CH$_2$, C-2 of alkyl chain), 29.6 (CH$_2$, C-3 of alkyl chain), 25.5(CH$_2$, C-4 of alkyl chain), 22.3 (CH$_2$, C-5 of alkyl chain), 14.2 (tCH$_3$, C-6 of alkyl chain).

HR-ESI-MS + ve: *m/z* 237.2224 (C+, **c**alcd. for $C_{15}H_{29}N_2^+$ *m/z* 237.2325), *m/z* 321.3255 (C^++Hexyl; $C_{21}H_{49}N_2^+$); *m/z* 153.1261 (C^+ − Hexyl; $C_9H_{17}N_2^+$); **HR-ESI-MS –ve:** *m/z* 137.0174 (calcd. For $C_7H_5O_3^-$ *m/z* 137.0238); *m/z* 275.0570 ($C_{14}H_{11}O_6^-$, A_2^- + H).

2.5. Synthesis of 1,3-dihexylimidazolium 2-aminobenzoate (RTIL-3)

Sodium salt of *o*-aminobenzoic acid (**OAB**) was prepared, followed by ion exchange with [hhim]$^+$ [Br]$^-$ following the method described in Section 2.3. A hydrophobic waxy brown product (3) was obtained. Yield: 90%.

IR ν_{max} KBr cm^{-1}: 3432.2, 3375.7 (NH$_2$), 3138.1, 3073.6, (aromatic C—H stretching), 2957.9, 2927.5, 2857.4 (aliphatic C—H stretching due to octyl chain hydrogen), 1689.4 (conjugated C=O), 1566.6 (C=N imidazole ring), 1494.2 (C=C imidazole ring), 1297.3 (C—N), 1161.1 (C—C).

***^{1}H NMR* (DMSO-d_6, 500 MHz) δ ppm:** 9.49 (s, N-CH-N, 1H), 7.83 (s, H-4 & H-5, 2H), 7.71 (dd, $J = 8.0, 1.5$ Hz, H-2′, 1H), 6.90 (dd, $J = 8.0, 1.5$ Hz, H-4′, 1H), 6.49 (dd, $J = 8.0, 1.5$ Hz, H-3′, 1H), 6.34 (dd, $J = 8.0, 1.5$ Hz, H-5′, 1H), 4.18 (br. s, 4H), 1.78 (br. s, CH$_2$- CH$_2$N, 4H), 1.26 (broad singlet, CH$_2$ x 4), 0.85 (br. s, 2 x terminal CH$_3$, 6H).

***^{13}C NMR* (DMSO-d_6, 125 MHz) δ ppm:** 172.2 (-COO$^-$), 150.5 (C—N anion), 136.7 (N-C=N imidazole ring), 132.1 (Anion C—H, C-4′), 129.7 (anion C—H, 6′), 122.9 (imidazole C-4 and C-5), 121.8 (anion C—H C-1′), 115.4 & 114.0 (Anion C—H, C-3′ and 5′), 49.2 (N-CH$_2$, C-1 of alkyl chain), 30.9(CH$_2$, C-2 of alkyl chain), 29.7 (CH$_2$, C-3 of alkyl chain), 25.5 (CH$_2$, C-4 of alkyl chain), 22.3 (CH$_2$, C-5 of alkyl chain), 14.2 (terminal CH$_3$, C-6 of alkyl chain).

HR-ESI-MS + ve: *m/z* 237.2224 (C+, **c**alcd. for $C_{15}H_{29}N_2^+$ *m/z* 237.2325), **HR-ESI-MS –ve:** *m/z* 136.0374 (A$^-$ calcd. For $C_7H_6NO_2^-$ *m/z* 136.0398); *m/z* 509.3118 [CA_2^-, $C_{29}H_{41}N_4O_4$]$^-$.

2.6. Synthesis of 1,3-dihexylimidazolium 4-aminobenzoate (RTIL-4)

Sodium salt of *p*-aminobenzoic acid (PABA) was prepared, followed by ion exchange with [hhim]$^+$ [Br]$^-$ following the method described in Section 2.3. A hydrophobic waxy dark brown product was obtained. Yield: 90%.

IR ν_{max} KBr cm^{-1}: 3431.6, 3420.2 (Aromatic NH$_2$), 3132.2, 3066.2 (aromatic C—H stretching), 2957.5, 2930.6, 2858.3 (aliphatic C—H stretching due to octyl chain hydrogen), 1604.2 (Conjugated C=O), 1562.4 (C=N imidazole ring), 1463.1 (C=C imidazole ring), 1376.8 (C—O), 1301.4 (C—N), 1163.2 (C—C).

***^{1}H NMR* (DMSO-d_6, 500 MHz) δ ppm:**: 9.39 (s, N-CH-N, 1H), 7.64 (br. s, H-4 & H-5 imidazole ring, 2H), 7.19 (br. s, H-2′ & H-6′ anion, 4H), 6.91 (br. s, H-3′ & H-5′ anion, 4H), 4.17 (br. s, N-CH$_2$, 4H), 1.69 (s, CH$_2$- CH$_2$N, 4H), 11.26 (broad singlet, CH$_2$ x 6, 12H), 0.85 (br. s, terminal CH$_3$, 6H).

***^{13}C NMR* (DMSO-d_6, 125 MHz; δ in ppm):** 122.92 (imidazole C-4 & C-5), 49.29 (CH$_2$, C-1 of alkyl chain), 46.44 (CH$_2$, C-1 of alkyl chain), 31.13 (CH$_2$, C-2 of alkyl chain), 30.99 (CH$_2$, C-2 of alkyl chain), 29.71 (CH$_2$, C-3 of alkyl chain), 26.04 (CH$_2$, C-4 of alkyl chain), 25.58 (CH$_2$, C-4 of alkyl chain), 22.44 (CH$_2$, C-5 of alkyl chain), 22.34 (CH$_2$, C-5 of alkyl chain), 14.30 (terminal CH$_3$, C-6 of alkyl chain), 14.25 (terminal CH$_3$, C-6 of alkyl chain). *Note:* N-C=N imidazole ring and carbon-based of anion could not be observed due to the exceptionally low sample quantity. Furthermore, the respective ^{1}H NMR was conducted with the same sample tube and observed according to the expected molecular structure.

HR-ESI-MS + ve: *m/z* 237.2224 (C+, **c**alcd. for $C_{15}H_{29}N_2^+$ *m/z* 237.2325), *m/z* 321.3255 (C^++Hexyl; $C_{21}H_{49}N_2^+$); *m/z* 153.1406 (C^+ − Hexyl; $C_9H_{17}N_2^+$); **HR-ESI-MS –ve**: *m/z* 136.0384 (A$^-$calcd. For $C_7H_6NO_2^-$ *m/z* 136.0398); *m/z* 509.3131 [$C_{29}H_{41}N_4O_4$]$^-$.

2.7. Electrical measurement of RTILs

Electrical conductivities of the RTILs **1–4** were recoded on a Hanna (probe model HI763100) conductivity meter at ambient temperature. Each sample was prepared in ethanol with varying molar concentrations. GLP Standard: 0 μS/cm, 12.88 mS/cm; Offset: 0.00 μS/cm, C.F. (cm^{-1}): 1.063; T. Coef (%/°C): 1.90; T. Ref (°C): 2; The results are listed in Table S1 (*Supporting information*).

2.8. Rheological studies of RTILs

The studies were performed using a Brookfield DV-III rheometer. The spindle selected for measurements was Spindle 0. The selection of spindles was based on the % torque limits of 10–100%. The prepared ionic liquid was used as is, without any dilution, for the rheology study. The volume of sample used was 16 mL as required by the UL Adapter spindle. The sample was set on hold for 5 min to equilibrate before each run. For each run, the % torque, viscosity, shear stress, and strain rate were recorded at different speeds (rpm). The data obtained were used in rheological modeling.

Rheologicak data could be evaluated using several models to obtain insight into the flow properties of the substance under study. Rheological models can be categorized as empirical (e.g., power law model), structural (e.g., Casson model), and theoretical (e.g., Newtonian) models. These models can be divided into two further types viz. time-independent and time-dependent models. In this study rheological data were processed using the Newtonian, Bingham, Power law, and

Casson models, which are time-independent models. The equations used for the models are as follows:

$$\text{Newtonian equation}: \tau = \eta D$$

$$\text{Bingham equation}: \tau = \tau_0 + \acute{\eta} D$$

$$\text{Casson}: \sqrt{\tau} = \sqrt{\tau_o^c} + \sqrt{\eta^c D}$$

$$\text{Power law}: \tau = kD^p$$

where τ $(Pa)$is used to represent shear stress and D corresponds to shear rate (s^{-1}). For the Newtonian equation, the term η is the viscosity (Pa.s). The terms τ_0 and $\acute{\eta}$ in the Bingham equation are the yield stress and Bingham plastic viscosity, respectively. The term τ_o^c is Casson yield stress and η^c is Casson plastic viscosity, where k and p in the power law are the consistency index and flow index.

2.9. General method for 4H-chromene derivatives using Knoevenagel-Michael-cyclocondensation

A mixture of dimedone (9 mmol), aromatic aldehyde (9 mmol), malononitrile (9 mmol) and RTIL (2% mol, dried at 70 °C in vacuum for 48 h before use) was refluxed in a suitable amount of ethanol. The reaction was monitored through TLC hexane-ethyl acetate (8:2). Upon completion, the reaction mixture was cooled to room temperature, the solvent was evaporated under vacuum and the product precipitated as a solid upon the addition of cold water. The precipitates were filtered and washed with water. To obtain pure products (**1a-1 h)** recrystallization was carried out using ethanol (95%). All compounds (**1a-1 h**) were characterized through co-TLC with authentic sample and physical data with those of previously documented literature [17,47,48]. To remove unreacted organic material from ionic liquid, it was treated with ethyl acetate.

2.10. General method for Knoevenagel cyclocondensation

Aromatic aldehyde (9 mmol) and malononitrile (9 mmol) were taken in suitable amounts of ethanol and stirred at reflux. TLC after 5 min confirmed the completion of the reaction. Solvent evaporation followed by precipitation with water yielded α-cyanoacrylates (**2a-2j**) in excellent yields (Table S4, *Supporting information*). The isolated products were compared with authentic samples through TLC (hexane-ethyl acetate) and comparison with physical data formerly reported in the literature confirmed the product formation [11,12,47,48].

2.11. Recycling of RTILs after reaction

In Sections 2.9 and 2.10, after removal of the solid product, the water and RTIL mixture was treated with ethyl acetate, resulting in three layers, RTIL in the middle. After removal of both water and ethyl acetate, the RTIL was again treated with ethyl acetate to remove unreacted organic reactants followed by drying.

3. Results & discussion

3.1. Synthesis and characterization of RTILs (1–4)

Using a two-step protocol by Dzyuba et al. [46], four C_2-symmetrical 1,3-dihexylimidazolium-based RTILs **1–4** were prepared. Metathesis of dihexylimidazolium with naturally occurring aromatic carboxylate anions containing polar moieties such as hydroxyl or amino groups in the C-2 or C-4 position makes them halide free, i.e., third generation RTILs. Two equivalents of imidazole were quaternized using hexylbromide in the presence of one equivalent of sodium hydride in THF following the Dzyuba et al. [46] method. The next and crucial step is the introduction of the desired anion. Sodium benzoates are obtained through the reaction of substituted benzoic acids with aqueous sodium bicarbonate solution. Upon mixing and stirring anion and cation solutions at room temperature, ion exchange occurs within half an hour, and sodium halide separates and RTILs result in excellent yields (Scheme 1). The newly formed RTILs **1–4** showed very exceptional solubility behaviour. They are easily soluble, miscible with ethanol, methanol, DMSO, chloroform and dichloromethane and insoluble in water, ethyl acetate, n-hexane and diethyl ether. We utilized this property for the separation of inorganic or organic impurities from mixtures and to recycle RTILs.

We used ^{1}H and ^{13}C NMR spectroscopy, FTIR, and ESI-MS to characterize of newly synthesized RTILs **1–4**. There are distinct protons in the ^{1}H NMR spectra of each RTIL. A singlet at δ 9.0–10.0 was attributed to H-2 of imidazolium while two singlets (in sole cases both appear as one singlet) in the aromatic region for H-4 and H-5. Likewise, anions exhibit signals in aromatic regions. IL-2 shows a signal at δ 16.0 due to intramolecular H-bonding later supported by ESI-MS displaying anion-anion aggregation (A_2^-). In FTIR, a lower wavenumber medium intense signal at approximately 1600–1690 cm^{-1} is suggestive of conjugated carbonyl indicating the presence of carboxylate ions. Water is one of the impurities of even hydrophobic ionic liquids. The water was removed under high vacuum for a period of one week. ESI-MS was used to determine the mass of the ionic liquids, as described in Section 3.2.

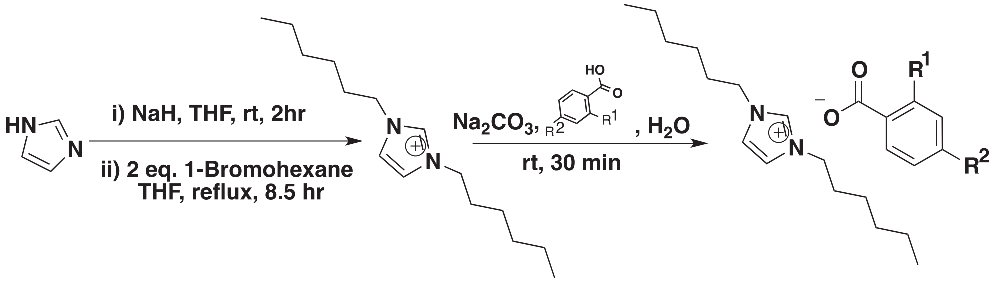

RTIL-1	$[hhim]^+ [OHB]^-$	$R^1 = OH$,	$R^2 = H$
RTIL-2	$[hhim]^+ [PHB]^-$	$R^1 = H$,	$R^2 = OH$
RTIL-3	$[hhim]^+ [OAB]^-$	$R^1 = NH_2$,	$R^2 = H$
RTIL-4	$[hhim]^+ [PAB]^-$	$R^1 = H$,	$R^2 = NH_2$

Scheme 1. Synthesis of RTILs 1–4

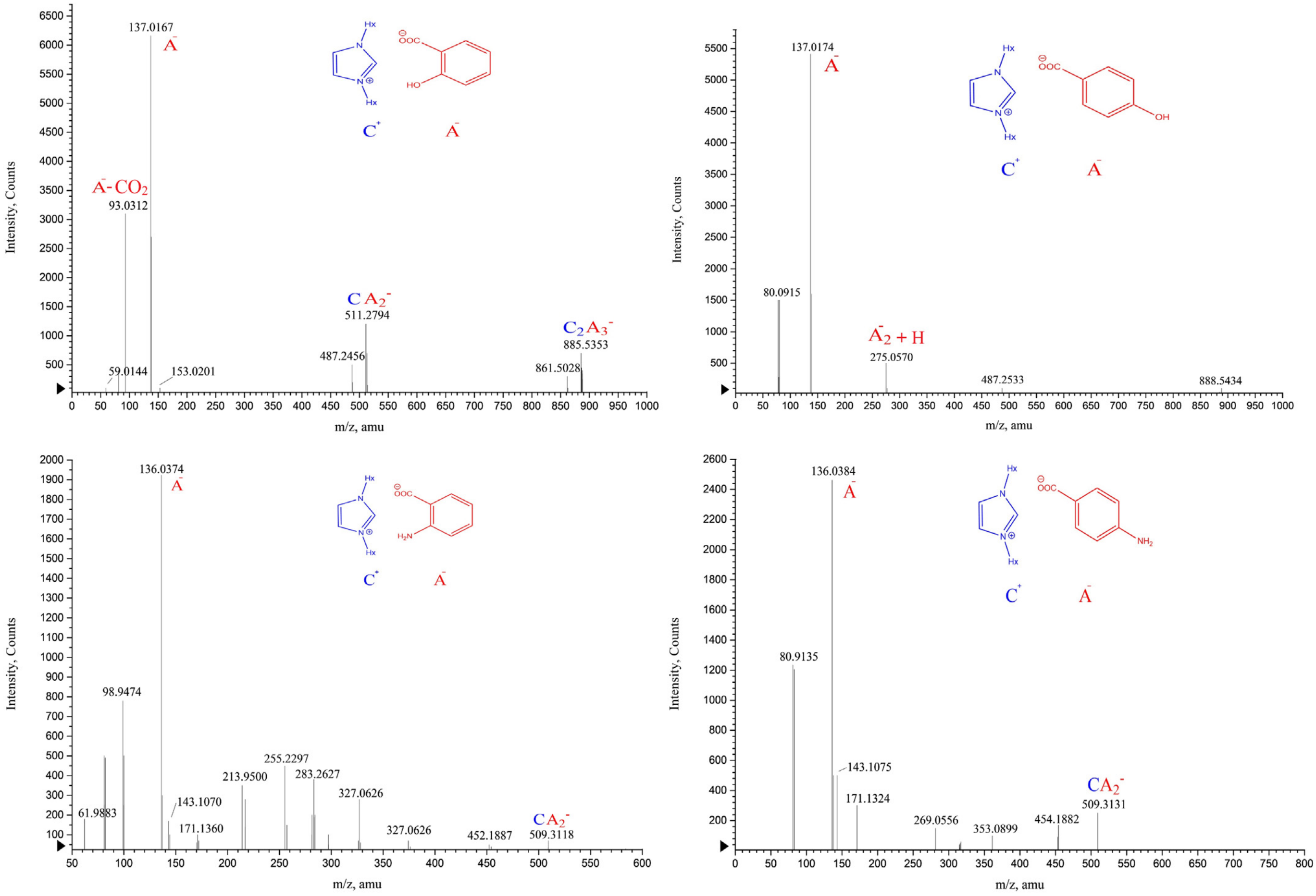

Fig. 2. **(a)** ESIMS (negative) spectrum of **RTIL-1**. **(b)** ESIMS (negative) spectrum of **RTIL-2**. **(c)** ESIMS (negative) spectrum of **RTIL-3**. **(d)** ESIMS (negative) spectrum of **RTIL-4**.

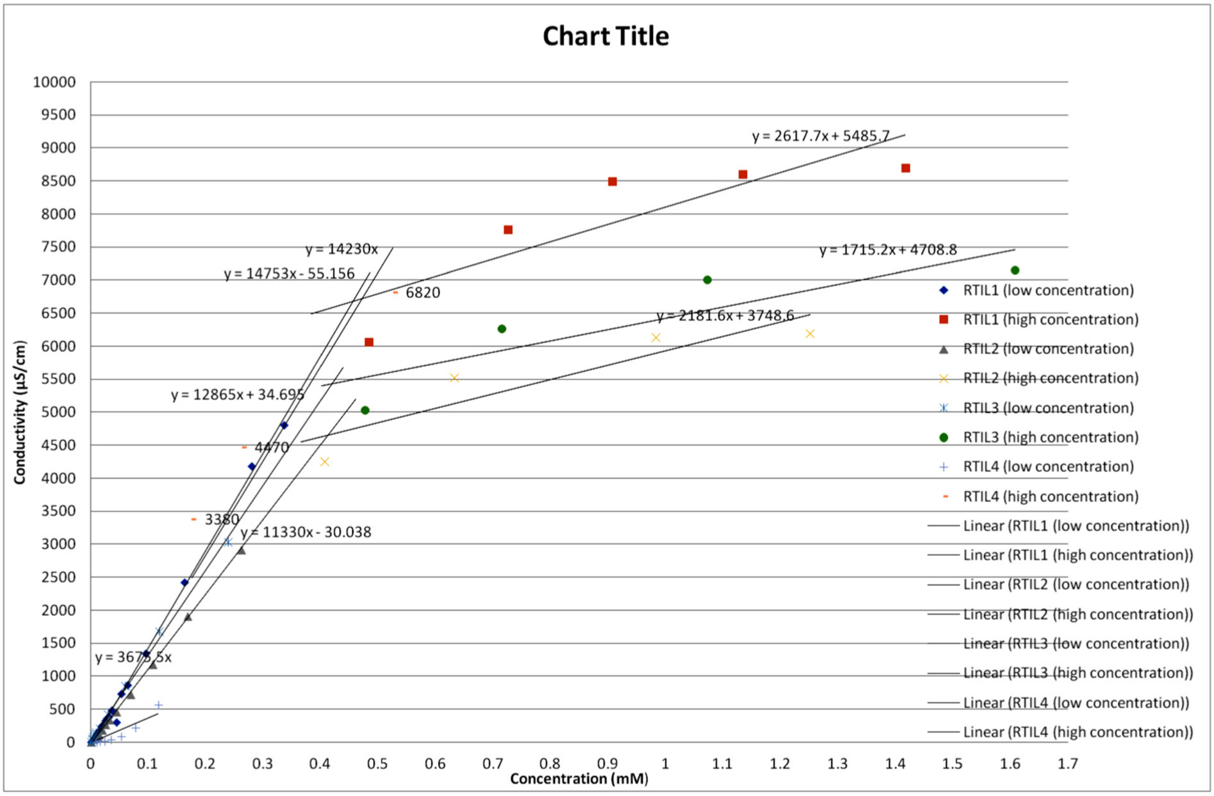

Fig. 3. Conductivity at varying concentrations of RTILs 1–3.

Table 1
Conductivity, critical aggregation concentration (**CAC**) and degree of ionization (α) of RTILs **1–3.**

RTIL	Conductivity (μScm^{-1})	CAC (mM)	α
1	6650	0.46	0.17
2	5400	0.42	0.19
3	4650	0.40	0.133

3.2. ESI-MS and polymeric aggregation of RTILs (1–4)

Four RTILs (**1–4**) were subjected to ESI-MS analysis to study their supramolecular aggregation performance. RTIL-**1**, −**3** and **4** exhibit cation-anion supramolecular polymeric aggregates in ESIMS negative mode (Fig. 2). On the other hand, the ESI-MS negative spectrum of RTIL-**2** displays anion-anion (Fig. 2b). The ESI-MS (negative) of **RTIL-1** exhibits cation-anion aggregates with decreasing intensity at *m/z* 511.2794 corresponding to $[CA_2]^{-\cdot}$ where C = cation (Dihexylimidazolium; $C_{15}H_{29}N_2^+$) and A = anion (2-hydroxybenzoate; $C_7H_5O_3^-$) and at *m/z* 885.5353 for $[C_2A_3]^-$.

We did not observe cation-anion aggregation in RTIL-**2** but a significant peak at *m/z* 275.0570 attributed to the $[A_2 + H]^-$, dianion of 4-hydroxybenzoate, which is in agreement with previously reported literature on anion-anion interactions [49]. Braga, D., et al. suggest that inter anion O-H….O- interaction arrange ions in space to furnish supramolecular anion-anion aggregation and reduce anion-anion electrostatic repulsion [49]. Mata and Molins theoretically demonstrated the formation of anionic dimers by oxoanions in the gaseous phase [50]. The anion-anion aggregation behaviour is observed only in *p*-hydroxybenzoate. This change in behaviour also affects the catalytic activity as described in the Section 3.6.

RTIL-**3** and RTIL-**4** display singly charged aggregates for $[CA_2]^-$ at *m/z* 509.3118 and *m/z* 509.3131, respectively. “A” corresponds to 2-aminobenzoate ($C_7H_6O_2N^-$) and 4-aminobenzoate ($C_7H_6O_2N^-$), while C = cation (Dihexylimidazolium; $C_{15}H_{29}N_2^+$).

On the other hand, ESI-MS positive not only exhibits a C^+ peak in each case with no cation-anion aggregation but also C-C_6H_{13} at *m/z* 153 fragments (Figs. S1, S2, S3, *vide Supporting information*). The results are suggestive of the effect of bulky symmetric cations on aggregate formation. Formerly, we noted the anion-anion interaction of 1-hexyl-3-methyl imidazolium $[hmim]^+$ with the four benzoates (used in this study as well) [11].

3.3. Conductivity measurments of RTILs 1–4

To further investigate aggregation behaviour and calculate the critical aggregation concentration (CAC) of RTILs, we recorded the electrical conductivity of RTILs as a function of concentration [51]. Initially, we

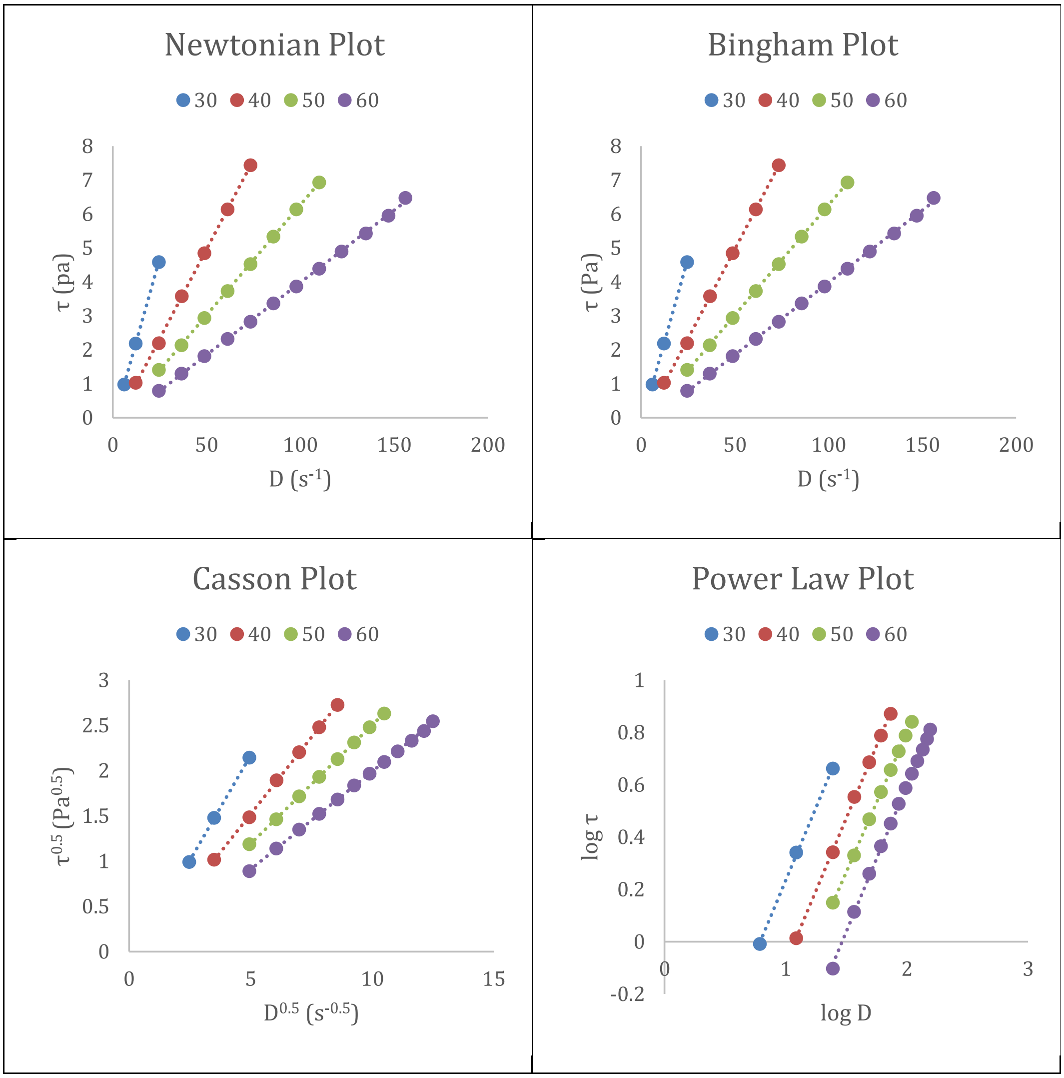

Fig. 4. Model fitting of Rheological data for **RTIL-1**.

observed a linear increase in conductivity with increasing concentration. However, upon further increases concentration we witnessed deviations from linear behaviour due to increased viscosity that reducing charge carrier mobility (Fig. 3). The reduction in mobility of charge carriers at higher concentrations again deviates and lowers conductivity, supporting aggregate formation. The highest deviation exhibits the "CAC" value demonstrated in Fig. 3 and Table 1. In addition, the degree of ionization (α) of the aggregates was calculated according to method reported by Wang et al. [51].

Fig. 3 demonstrates the non-linear variation of the conductivity versus concentration plot of RTILs **1–4**. As cations are common among all RTILs investigated in the present study, the variations are mainly attributed to the anions. RTIL-2 showed relatively lower conductivity values and higher α, supporting anion-anion aggregation observed in negative ESIMS (Fig. 2b).

3.4. Rheology of RTILs

Ionic liquids have a tremendous scope in the field of catalysis. They can also be used as solvents and are aimed at replacing traditional organic solvents in the field of separation sciences and synthesis [52]. The study of the rheological properties of ionic liquids is essential for their effective utilization. The ionic liquids synthesized (RTIL **1–3**) in this study were subjected to rheological experiments at different temperatures. The obtained data for **RTIL-1** were evaluated using rheological models and their plots are shown in Fig. 4. The plots for **RTIL-3** and **RTIL-2** are shown in Figs. 5 and 6 respectively. The model parameters obtained for the synthesized ionic liquids are reported in Table S2 (Supporting information). It was observed that the correlation coefficients obtained for the selected models were quite high which inferred that the models explained the rheological data quite well.

The shear stress varied proportionally with the shear rate. This behaviour is specific to Newtonian fluids. However, Newtonian plots showed a nonzero intercept, indicating that the behaviour of the ionic liquids can be explained using the Bingham model.

The Bingham model is used for fluids, which show high resistance to initial flow. Once the flow starts, the sheer stress can be correlated to the strain rate by either linear (Newtonian) or nolinear (non-Newtonian) proportions. A measure of the resistance offered by a fluid to its initial flow is termed the yield stress. The value is usually positive for most of the substances, such as toothpastes, ketchups etc. Although high values of the correlation coefficient were observed between shear stress and the strain rate, the model produced negative values for yield stress, τ_0, as shown in Table S2 (Supporting information). The negative value of yield stress is normally considered an unrealistic solution of a model indicating ineptness of the model [53].

The Casson model showed high values for the correlation coefficient indicating a good fit between the experimental data and model

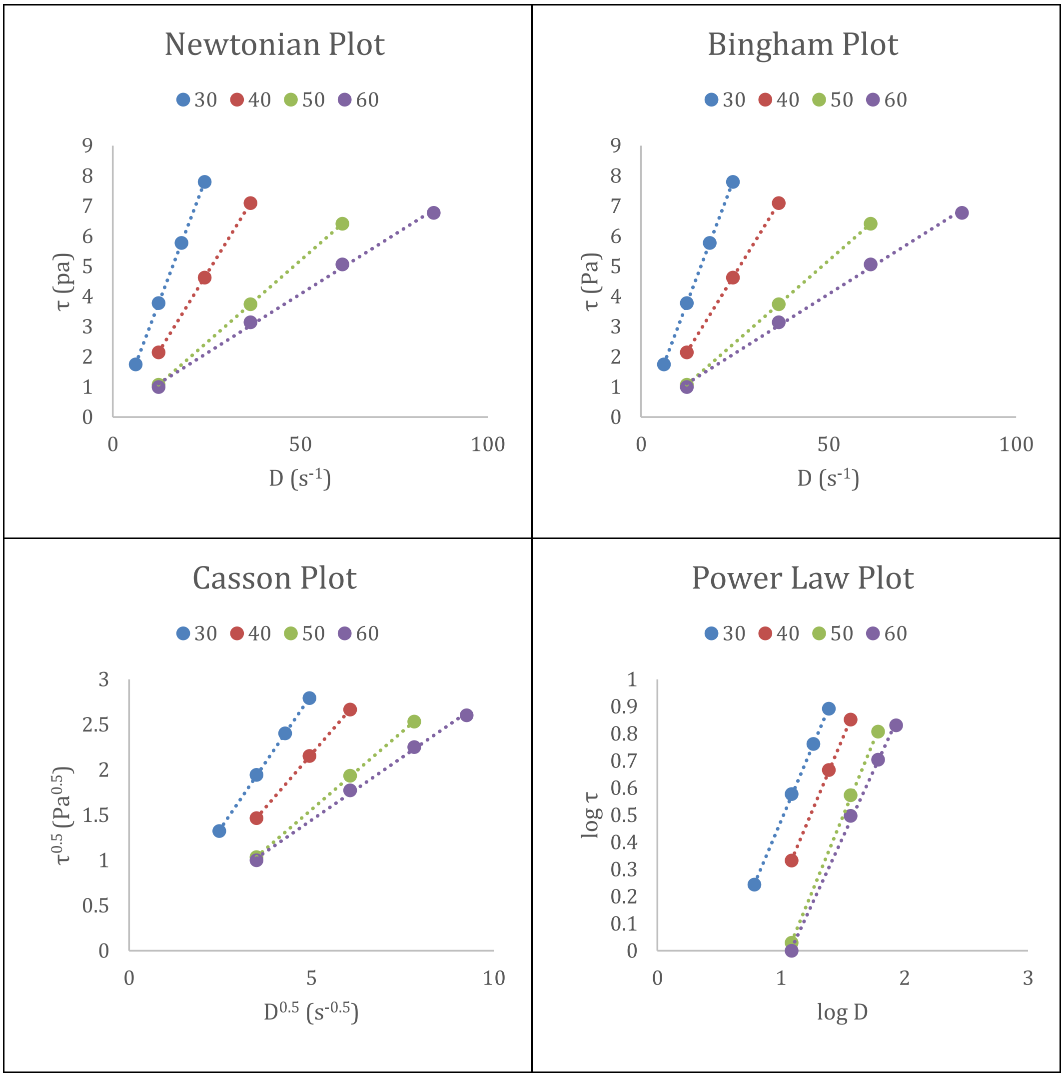

Fig. 5. Model fitting for Rheological data for **RTIL-2**.

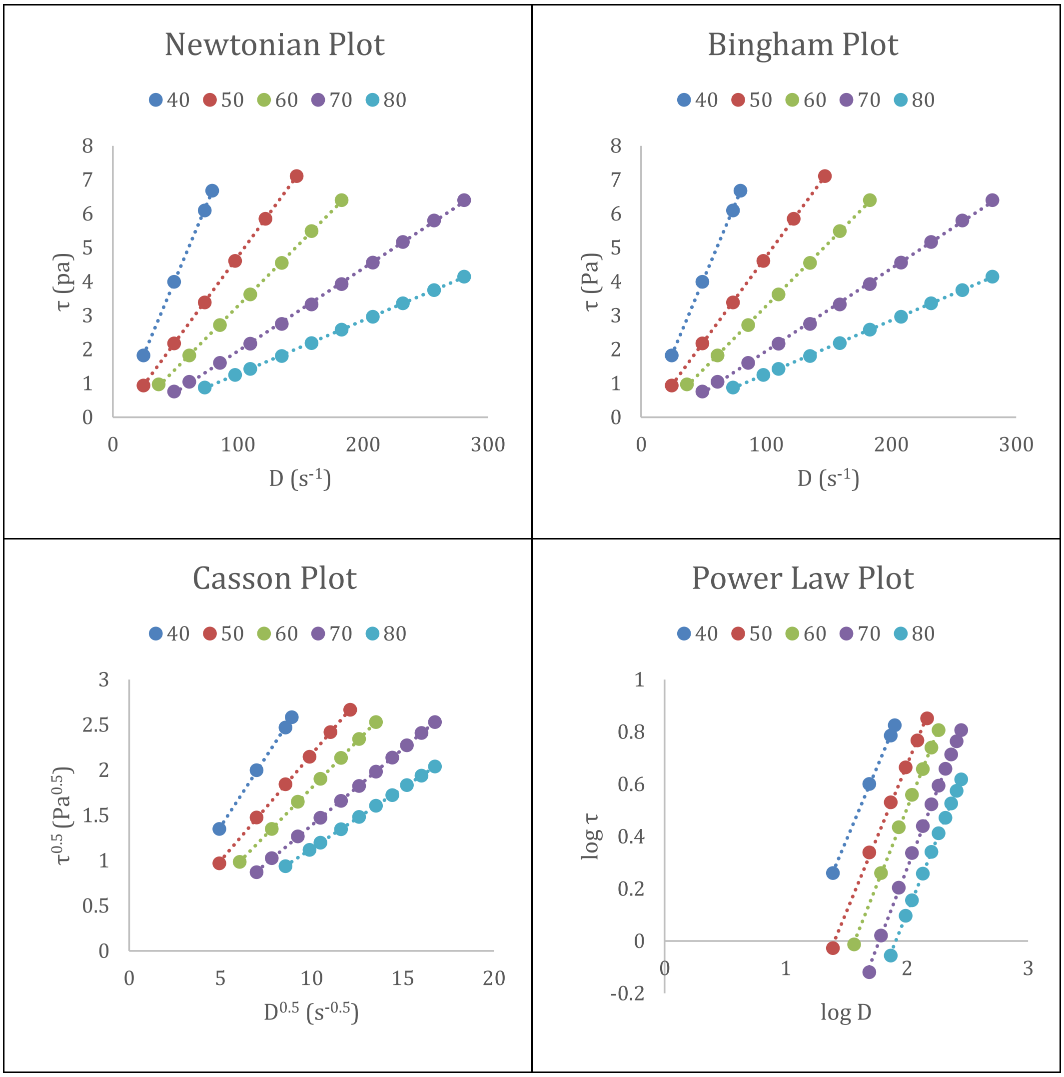

Fig. 6. Model fitting for Rheological data for **RTIL-3**.

assumptions. The Casson yield stress, τ_o^c, values obtained were positive and were negligible as compared to yield stress values for common products shown in Table S3 (Supporting information). The Casson plastic viscosity values obtained for ionic liquids were quite close to the average viscosities determined experimentally.

The power law model is an empirical model with the capability to differentiate Newtonian fluids from non-Newtonian fluids. The model parameter p, the flow index, is a dimensionless parameter that classifies a fluid as Newtonian if $p = 1$. A fluid is said to exhibit shear thinning behaviour if $p < 1$ and is classified as pseudoplastic, whereas, for $p > 1$ the fluid is termed as dilatant, which shows shear thickening behaviour. The

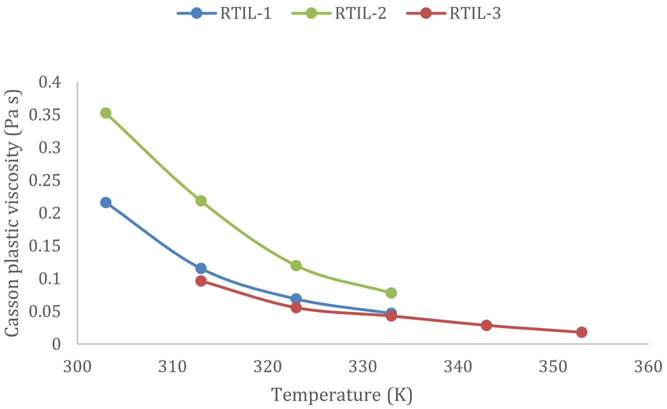

Fig. 7. Effect of temperature on ionic liquid viscosity.

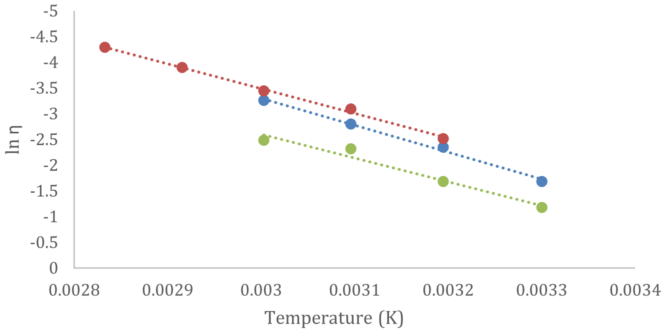

Fig. 8. Arrhenius plots of ionic liquids for activation energy of flow.

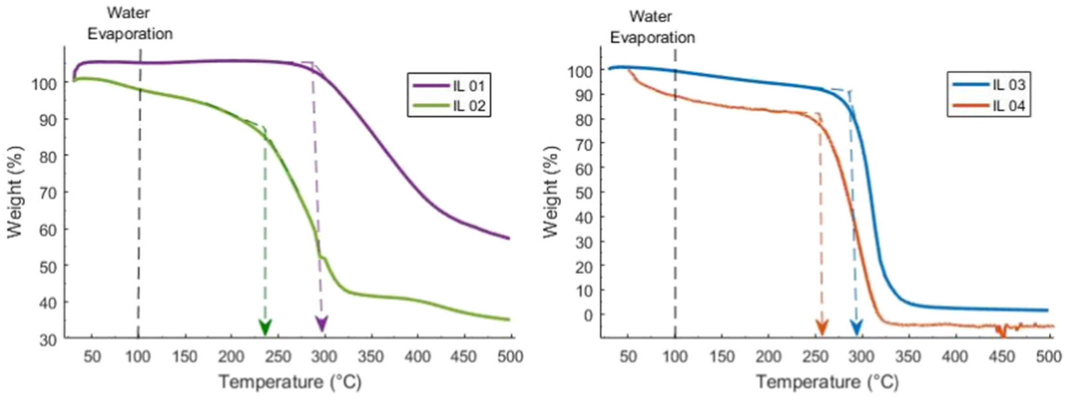

Fig. 9. TGA data of **RTILs 1–4.**

Scheme 2. Synthesis of *4H*-chromene-3-carbonitrile using RTILs

values of p obtained for ionic liquids under study ranged from 0.98 to 1.20. The values were quite close to 1 and lead to the conclusion that the ionic liquids possessed flow properties similar to those of the Newtonian fluids.

Figs. 4, 5 and 6 show that the slope of the shear stress vs strain rate plots decreased with an increasing temperature. Fig. 7 shows a plot of Casson plastic viscosity obtained for **RTIL-1**, **RTIL-3**, and **RTIL-2** against temperature. The plot shows a nonlinear inverse relationship between viscosity and temperature.

A plot of the logarithm of viscosity against the temperature inverse can be used for the determination of activation energy for Newtonian fluids with constant viscosity. The ionic liquids under study were found to be Newtonian; hence, the Arrhenius equation was applied on to the experimental data to obtain the activation energy for the flow.

The average experimental viscosity was used to construct the plots, as shown in Fig. 8. The activation energy determined from the slope of the Arrhenius plot was 43.5 kJ mol^{-1} for **RTIL-1**, 40.0 kJ mol^{-1} for **RTIL-3**, and 38.5 kJ mol^{-1} for **RTIL-2**. The activation energy for water flow within the range of working temperature range (303–353 K) is 14.9 kJ mol^{-1} [54], which is significantly lower than that of the ionic liquids under study.

$$\ln \eta = \mathrm{B} + \frac{\mathrm{E_a}}{\mathrm{R}}\frac{1}{\mathrm{T}}$$

Table 2
Optimization of reaction conditions for the synthesis of *4H*-chromene-3-carbonitrile[a].

Entry	RTIL	Solvent	% RTIL	Yield%[b]	Time (min)
1	1	Ethanol	2	40.48	300
2	1	Ethanol	2	69.34	60
3	1	Ethanol	4	72.89	45
4	1	Ethanol	6	72.96	45
5	1	Ethanol	8	74.11	40
6	2	Ethanol	2	61.58	120
7	2	Ethanol	4	68.11	120
8	2	Ethanol	6	68.39	100
9	2	Ethanol	8	69.01	90
10	3	Ethanol	2	77.65	30
11	**3**	**Ethanol**	**4**	**83.06**	**30**
12	3	Ethanol	6	83.45	30
13	3	Ethanol	8	84.91	30
14	4	Ethanol	2	76.39	30
15	4	Ethanol	4	82.06	30
16	4	Ethanol	6	83.79	30
17	4	Ethanol	8	85.82	25

[a] 2-amino-7,7-dimethyl-4-(4-nitrophenyl)-5-oxo-5,6,7,8-tetrahydro-4H-chromene-3-carbonitrile. Reaction Conditions: 4-nitrobenzaldehyde (9 mmol), malononitrile (9 mmol), dimedone (9 mmol), RTILs in ethanol.

[b] Isolated yield.

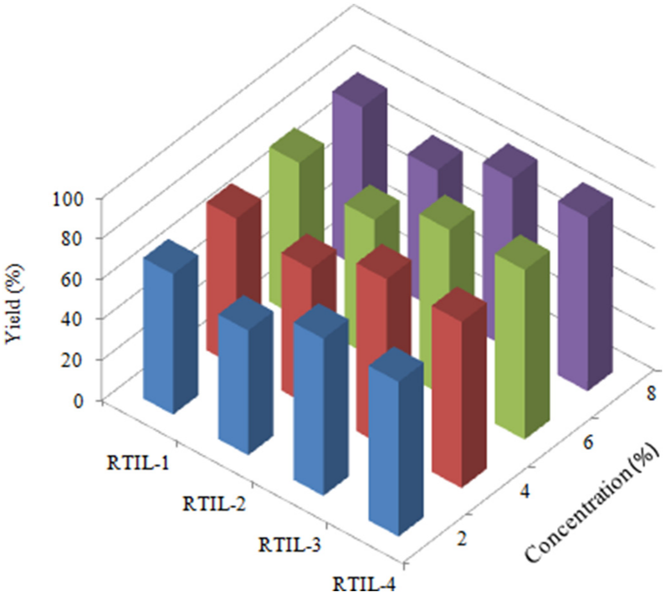

Fig. 10. Optimization of reaction conditions for the synthesis of *4H*-chromene-3-carbonitrile.

Scheme 3. Synthesis of *α-cyanoacrylates* using RTILs

3.5. Thermal stability of RTILs 1–4

The thermal stabilities of RTILs 1–4 were examined through thermogravimetric analysis (TGA). For characterization of RTILs, T_{onset} was recorded. T_{onset} was set from 200 to 400 °C. The degradation temperatures were found to be 295 °C, 230 °C, 260 °C and 290 °C for RTIL1–4, respectively (Fig. 9). This shows the significant role of the type and orientation of substituents on the benzoate anion on the thermal stability of RTILs.

3.6. Catalytic activity of RTILs for synthesis of 4H-chromene carbonitrile

Initially, we carried out the reaction at room temperature using RTIL-1 (2%) in water at room temperature without any base (Scheme 2).

Table 3
Substrate scope of Catalyst (**RTIL-3**) using optimal conditions.

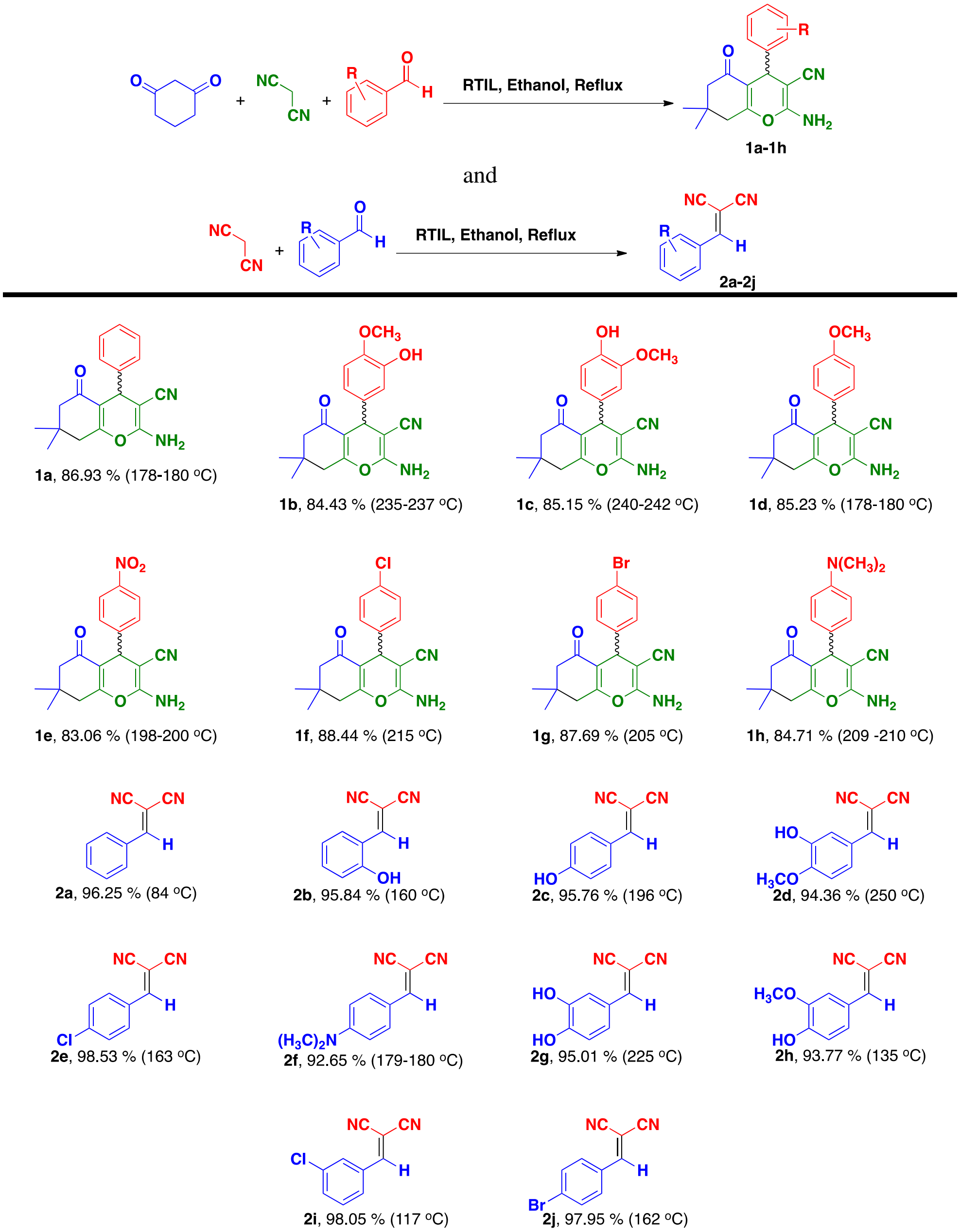

1a, 86.93 % (178-180 °C)
1b, 84.43 % (235-237 °C)
1c, 85.15 % (240-242 °C)
1d, 85.23 % (178-180 °C)
1e, 83.06 % (198-200 °C)
1f, 88.44 % (215 °C)
1g, 87.69 % (205 °C)
1h, 84.71 % (209 -210 °C)
2a, 96.25 % (84 °C)
2b, 95.84 % (160 °C)
2c, 95.76 % (196 °C)
2d, 94.36 % (250 °C)
2e, 98.53 % (163 °C)
2f, 92.65 % (179-180 °C)
2g, 95.01 % (225 °C)
2h, 93.77 % (135 °C)
2i, 98.05 % (117 °C)
2j, 97.95 % (162 °C)

Table 4
Correlation of supramolecular polymeric aggregation in **RTIL 1–4** and catalytic activity in Knoevenagel condensation and *4H*-chromene-3-carbonitrile synthesis.

IL	% Abundance of negatively charged aggregates			Catalytic activity			
				Knoevenagel condensation		*4H*-Chromene synthesis	
	$[A_2 + H]^-$	CA_2^-	$C_2A_3^-$	Time (min)	% Yield	Time (hr)	% Yield
RTIL-1	0	25	15	1	90.31	5	72.89
RTIL-2	10	0	0	1	88.76	6	68.11
RTIL-3	0	5	0	1	96.37	4	83.06
RTIL-4	0	12.5	0	1	93.92	4	82.06

Despite the hydrophobicity of ILs, water was used due to phase transfer catalytic behaviour of RTILs. No reaction was detected after 24 h. Therefore, we subjected the reaction in ethanol on reflux but only 40.48% of the product was obtained after 5 h (Entry-1; Table 2). The refluxed reaction mixture (in ethanol) yielded a better product within 30 min. Upon increasing the % concentration of RTIL, an increase in the % yield was observed. The performance of RTILs 2–4 was then explored (Fig. 10). RTIL-2 took longer times, and reduced yields were obtained. RTIL-3, (**$[hhim]^+$ $[OAB]^-$),** appeared to be an excellent catalyst for the synthesis of *4H*-chromene-3-carbonitrile among all tested RTILs (**1–4**).

To compare the effect of the catalytic activity of hydrophobic RTILs with previous results [1], we probed Knoevenagel condensation (Scheme 3). Similarly, instead of water, ethanol proved to be a better solvent, and RTIL-3 was verified to be the best catalyst (Table S4, *Supporting Information*). These results suggest the role of the anion and supramolecular polymeric aggregation of RTIL in catalytic activity.

The scope of different aromatic aldehydes using optimal conditions was investigated. Reactions with different substituted aromatic aldehydes resulted in moderate to high yields in both in *4H*-chromene derivatives and Knoevenagel condensation (Table 3).

3.7. Correlation of supramolecular polymeric aggregation and catalytic activity

A remarkable relationship between supramolecular polymeric aggregation of RTILs and catalytic activity was observed and found to be in agreement with previous observations (Table 4) [1]. Earlier, two types of ionic interactions were observed in all examined ILs, i.e., cation-anion and anion-anion interactions and a decrease in catalytic activity were observed with increased anion-anion interactions. Table 1 clearly indicats that the only **RTIL-2** exhibiting anion-anion interactions shows comparatively poor activity. On the other hand, **RTIL-3** with the least supramolecular polymeric aggregation proves to be an excellent catalyst for both reactions studied.

3.8. Catalyst recyclability

Despite the cost of RTILs, an enormous benefit of these unique materials is their recyclability, especially in the case of hydrophobic RTILs that can easily be purified by treatment with water to remove inorganic byproducts. After every run, **RTIL-3** was recycled and reused in the subsequent reactions four times without losing its efficiency and activity.

4. Conclusion

Noncovalent interactions, among molecules or ions result in supramolecular self-assemblies. Hydrogen bonding aggregation and neutral interionic aggregation are not compatible with our findings; we may opt for charged ionic interactions for aggregation.

It was concluded from the results that the type of cation and anion influences the extent of supramolecular polymeric aggregates, which can be used to determine the catalytic performance of an ionic liquid in organic reactions. Rheological experiments revealed that RTILs 1–4 are Newtonian and aggregates were formed due to electrostatic interactions instead of *H*-bonding. In addition, the RTIL was recycled five times without a significant drop in catalytic activity and change in chemical structure of RTILs. Recyclability reduces cost for these industrially important reactions and makes it effective for large-scale industrial use. Moreover, 1,3-dialkylimidazolium-based ionic liquids are already being sold in 1 to 5 kg of packaging, while reagents to make the anions are easily available. Ion pairing (self-assembled aggregates) has a direct influence on the rate and mechanism of organic reactions. Previously, the high reaction rate in C—C bond formation reactions (Knoevenagel condensation, Robbinson annulation) was attributed to imidazolidene carbenes due to the use of inorganic bases as catalysts. We have observed that no inorganic base is required, as RTILs can serve as base catalysts. The use of ILs as reaction media or catalysts is now very common, but the use of hydrophobic ILs as catalysts for organic reactions is rare.

CRediT authorship contribution statement

IA Hashmi, and FI Ali conceived the present idea, designed and directed the project. S Muhammad, MN Javed, carried out synthesis and purification. AA Waseem and M.Amir performed Rheological data. S Muhammad, F Rafique, K. Riyaz and A Ilyas measured and analyzed conductivity experiments. SG Musharraf and *A. Bari* performed spectroscopy. S. Muhammad, MN Javed, SG Musharraf, *A. Bari* and FI ALI performed characterization. SJ Mehmood and MN Javed recoded TGA data. All Authors equally contributed to interpretation of the results, discussions and writing the manuscript.

Declaration of competing interest

The authors declare that they have no known competing financial interests or personal relationships that could have appeared to influence the work reported in this paper.

Acknowledgment

The authors extend their appreciation to the Deanship of scientific research at King Saud University for funding this work through research group no RG-1440-009.

Appendix A. Supplementary data

Supplementary data to this article can be found online at https://doi.org/10.1016/j.molliq.2020.114503.

Table 5
Catalytic evaluation of present study with some reported procedures for the reaction of dimedone, malononitrile and benzaldehyde.

Sr no.	Catalyst (mol/g)	Condition	Time (min)	Yield (%)	Ref
1	Ba(OTf)2	PEG-Water (50–50), rt	30	96	[13]
2	[cmmim]Br	Solvent free, 115 °C	10	93	[17]
3	Na_2SeO_4	H2O/ EtOH (1:1), Reflux	180	90	[17]
4	N-Methylimidazole	H2O, rt	13	80	[17]
5	RTIL-3	Ethanol, Reflux	30	86.93	Our work

References

[1] F. Rodriguez-Llansola, J.F. Miravet, B. Escuder, Supramolecular catalysis with extended aggregates and gels: inversion of Stereoselectivity caused by self-assembly, Chemistry, A European Journal 16 (2010) 8480–8486.

[2] L. Leclercq, A.R. Schmitzer, Supramolecular effects involving the incorporation of guest substrates in imidazolium ionic liquid networks: recent advances and future developments, Supramol. Chem. 21 (2009) 245–263.

[3] J. Dupont, On the solid, liquid and solution structural organization of imidazolium ionic liquids, J. Braz. Chem. Soc. 15 (2004) 341–350.

[4] A.R. Gholap, K. Venkatesan, T. Daniel, R.J. Lahoti, K.V. Srinivasan, Ultrasound promoted acetylation of alcohols in room temperature ionic liquid under ambient conditions, Green Chem. 5 (2003) 693–696.

[5] J. Fraga-Dubreuil, K. Bourahla, M. Rahmouni, J.P. Bazureau, J. Hamelin, Catalysed esterifications in room temperature ionic liquids with acidic counteranion as recyclable reaction media, Catal. Commun. 3 (2002) 185–190.

[6] J.A. Boon, J.A. Levisky, J.L. Pflug, J.S. Wilkes, Friedel-crafts reactions in ambient-temperature molten salts, J. Organomet. Chem. 51 (1986) 480–483.

[7] M.J. Earle, S.P. Katdare, K.R. Seddon, Paradigm confirmed: the first use of ionic liquids to dramatically influence the outcome of chemical reactions, Org. Lett. 6 (2004) 707–710.

[8] A.R. Gholap, K. Venkatesan, T. Daniel, R.J. Lahoti, K.V. Srinivasan, Ionic liquid promoted novel and efficient one pot synthesis of 3,4-dihydropyrimidin-2-(1*H*)-ones at ambient temperature under ultrasound irradiation, Green Chem. 6 (2004) 147–150.

[9] J.C. Hsu, Y.H. Yen, Y.H. Chu, Baylis–Hillman reaction in [bdmim][PF$_6$] ionic liquid, Tetrahedron Lett. 45 (2004) 4673–4676.

[10] L. Hao, Y. Zhao, B. Yu, Z. Yang, H. Zhang, B. Han, X. Gao, Z. Liu, Imidazolium-based ionic liquids catalyzed formylation of amines using carbon dioxide and phenylsilane at room temperature, ACS Catal. 5 (2015) 4989–4993.

[11] S. Muhammad, M.N. Javed, F.I. Ali, A. Bari, I.A. Hashmi, Supramolecular polymeric aggregation behavior and its impact on catalytic properties of imidazolium based hydrophilic ionic liquids, J. Mol. Liq. 300 (2020)https://doi.org/10.1016/j.molliq.2019.112372.

[12] M.N. Javed, S. Muhammad, I.A. Hashmi, A. Bari, S.G. Musharraf, F.I. Ali, Newly designed pyridine and piperidine based ionic liquids: aggregation behavior in ESI-MS and catalytic activity in CC bond formation reactions, J. Mol. Liq. 272 (2018) 84–91.

[13] A. Kumar, S. Rao, An expeditious and greener one-pot synthesis of *4H*-chromenes catalyzed by Ba(OTf)2 in PEG-water, Green Chemistry Laetters and Reviews 5 (2012) 283–290.

[14] T. Welton, Room-temperature ionic liquids, solvents for synthesis and catalysis, Chem. Rev. 99 (1999) 2071–2083.

[15] Q. Zhang, S. Zhang, Y. Deng, Recent advances in ionic liquid catalysis, Green Chem. 13 (2011) 2619–2637.

[16] C. Yue, D. Fang, L. Liu, T.F. Yi, Synthesis and application of task-specific ionic liquids used as catalysts and/or solvents in organic unit reactions, J. Mol. Liq. 163 (2011) 99–121.

[17] A.R. Moosavi-Zare, M.A. Zolifgol, O. Khaledian, V. Khakyzadeh, M.D. Farhani, M.H. Beyzavi, H.G. Kruger, Tandem Knoevenagel–Michael–cyclocondensation reaction of malononitrile, various aldehydes and 2-naphthol over acetic acid functionalized ionic liquid, Chem. Eng. J. 248 (2014) 122–127.

[18] P. Kubisa, Ionic liquids as solvents for polymerization processes-progress and challenges, Prog. Polym. Sci. 34 (2009) 1333–1347.

[19] Z. He, P. Alexandridis, Nanoparticles in ionic liquids: interactions and organization, Phys. Chem. Chem. Phys. 17 (2015) 18238–18261.

[20] S. Muhammad, F.I. Ali, A. Aslam, V.U. Ahmad, A.N. Khan, Synthesis of thiosalicylate based hydrophobic ionic liquids and their applications in metal extraction from aqueous solutions, J. Chem. Soc. Pak. 37 (2015) 535–540.

[21] T.V. Hoogerstraete, B. Onghena, K. Binnemans, Homogeneous liquid-liquid extraction of metal ions with a functionalized ionic liquid, J. Phys. Chem. Lett. 4 (2013) 1659–1663.

[22] A.P. Rios, F.J. Hernandez-Fernandez, L.J.L. Sanchez, J.I. Moreno, C. Godinez, Removal of metal ions from aqueous solutions by extraction with ionic liquids, J. Chem. Eng. Data 55 (2010) 605–608.

[23] V.H. Choi, R. Verpoorte, Green solvents for the extraction of bioactive compounds from natural products using ionic liquids and deep eutectic solvents, Current openion in food science 26 (2019) 87–93.

[24] M.G. Freire, C.M.S.S. Neves, I.M. Marrucho, J.N.C. Lopes, L.P.N. Rebelo, J.A.P. Coutinho, High-performance extraction of alkaloids using aqueous two-phase systems with ionic liquids, Green Chem. 12 (2010) 1715–1718.

[25] J.G. Huddleston, H.D. Willauer, R.P. Swatloski, A.E. Visser, R.D. Rogers, Room temperature ionic liquids as novel media for 'clean' liquid-liquid extraction, Chem. Commun. 34 (1998) 1765–1766.

[26] T.Y. Cho, S.G. Yoon, S.S. Sekhon, C.H. Han. Effect of ionic liquids with different cations in I-/I3- redox electrolyte on the performance of dye-sensitized solar cells bull. Korean Chem. Soc., 32 (2011) 2058-2062.

[29] K. Xu, Nonaqueous liquid electrolytes for lithium-based rechargeable batteries, Chem. Rev. 104 (2004) 4303–4417.

[30] A. Balducci, Ionic liquids in lithium-ion batteries, in: B. Kirchner, E. Perlt (Eds.), Ionic Liquids II. Topics in Current Chemistry Collections, vol. 375, Springer, Cham, 2017.

[31] M. Watanabe, M.L. Thomas, S. Zhang, K. Ueno, T. Yasuda, K. Dokko, Application of ionic liquids to energy storage and conversion materials and devices, Chem. Rev. 117 (2017) 7190–7239.

[32] P. Wasserscheid, T. Welton, Ionic Liquids in Synthesis, Wiley-VCH Verlag GmbH & Co. KGaA, 2008.

[33] H. Olivier-Bourbigou, L. Magna, D. Morvan, Ionic liquids and catalysis: recent progress from knowledge to applications, Applied Catalysis A 373 (2010) 1–56.

[34] T. Welton, Ionic liquids: a brief history, Biophys. Rev. 10 (2018) 691–706.

[35] H.L. Ngo, K. LeCompete, L. Hargens, A.B. McEwen, Thermal properties of imidazolium ionic liquids, Thermochemica Acta 357-8 (2000) 97–102.

[36] S. Ahrens, A. Peritz, T. Strassner, Tunable aryl Al-kyl ionic liquids (TAAILs): the next generation of ionic liquids, Angew. Chem. Int. Ed. 48 (2009) 7908–7910.

[37] M. Koel, Physical and chemical properties of ionic liquids based on the dialkylimidazolium cation, Proc. Estonian Acad. Sci. Chem. 49 (2000) 145–155.

[38] A.A. Fannin Jr., L.A. King, J.A. Levisky, J.S. Wilkes, Properties of 1,3-dialkylimidazole chloride-aluminium chloride ionic liquids. 1. Ion interaction by nuclear magnetic resonance spectroscopy, J. Phys. Chem. 88 (1984) 2609–2614.

[39] G. Cravotto, L. Boffa, J.M. Leveque, J. Estager, M. Draye, W. Bonarth, A speedy one-pot synthesis of second-generation ionic liquids under ultrasound and/or microwave irradiation, Aust. J. Chem. 60 (2007) 946–959.

[40] S. Armakovic, S.J. Armakovic, M. Vranes, A. Tot, S. Godzuric, DFT study of 1-butyl-3-methylimidazolium salicylate: a third-generation ionic liquid, J. Mol. Model. 21 (2015) 246.

[41] R. Bini, O. Bortolini, C. Chiappe, D. Pieraccini, T. Siciliano, Development of cation/anion "interaction" scales for ionic liquids through ESI-MS measurements, J. Phys. Chem. B 111 (2007) 598–604.

[42] N.M. Vaghela, N.V. Satry, V.K. Aswal, Surface active and aggregation behavior of methylimidazolium-based ionic liquids of type [C**n**mim] [**X**], **n**=4, 6, 8 and [**X**]= Cl−, Br−, and I− in water, Colloid Polym. Sci. 289 (2011) 309–322.

[43] A. Shakeel, H. Mahmood, U. Farooq, Z. Ullah, S. Yasin, T. Iqbal, C. Chassagne, M. Muniruzzaman, Rheology of pure ionic liquids and their complex fluids: a review, ACS Sustain. Chem. Eng. 7 (2019) 13586–13626.

[44] G.L. Burrell, I.M. Burgar, F. Separovic, N.F. Dunlop, Preparation of protic ionic liquids with minimal water content and 15N NMR study of proton transfer, Phys. Chem. Chem. Phys. 12 (2010) 1571–1577.

[45] G.L. Burrell, N.F. Dunlop, F. Separovic, Non-Newtonian viscous shear thinning in ionic liquids, Soft Matter 6 (2010) 2080–2086.

[46] S.V. Dzyuba, R.A. Bartsch, New room-temprature ionic liquids C_2-symmetrical immidazolium cations, Chem. Commun. (2001) 1466–1467.

[47] H. Valizadeh, S. Vaghefi, One-pot Wittig and Knoevenagel reactions in ionic liquid as convenient methods for the synthesis of coumarin derivatives, Synth. Commun. 39 (2009) 1666–1678.

[48] J. Yang, S. Liu, H. Hu, S. Ren, A. Ying, One-pot three-component synthesis of tetrahydrobenzo [b] pyrans catalyzed by cost-effective ionic liquid in aqueous medium, Chin. J. Chem. Eng. 23 (2015) 1416–1420.

[49] D. Barga, F. Grepioni, J.J. Novoa, Inter-anion O-H$^-$…..O$^-$ hydrogen bond like interactions: the breakdown of the strength-length analogy, Chem. Commun. 34 (1998) 1959–1960.

[50] I. Mata, E. Molins, I. Alkorta, E. Espinosa, The paradox of hydrogen bonded anion-anion aggregates in oxoanions: a fundamental electrostatic problem explained in terms of electrophilic···nucleophilic interactions, J. Phys. Chem. A 119 (2015) 183–194.

[51] H. Wang, J. Wang, S. Shang, X. Xuan, Structural effects of anions and cations on the aggregation behavior of ionic liquids in aqueous solutions, J. Phys. Chem. B 112 (2008) 16682–16689.

[52] C.F. Poole, Ionic Liquids, in: I.D. Wilson (Ed.), Encyclopedia of Separation Science, Academic Press, Oxford 2007, pp. 1–8.

[53] V.C. Kelessidis, R. Maglione, C. Tsamantaki, Y. Aspirtakis, Optimal determination of rheological parameters for Herschel–Bulkley drilling fluids and impact on pressure drop, velocity profiles and penetration rates during drilling, J. Pet. Sci. Eng. 53 (2006) 203–224.

[54] G.D. Saravacos, Effect of temperature on viscosity of fruit juices and purees, J. Food Sci. 35 (1970) 122–125.